Dual-Band Horn Array Design Using a Helical Exciter for Mobile Satellite Communication Terminals

Young-Bae Jung, *Member, IEEE*, and Soon-Young Eom, *Member, IEEE*

***Abstract*—A horn array antenna is proposed for dual-band and dual-polarization operation. The array is optimally designed to be used as a feeder in mobile satellite terminals with a hybrid antenna (HA) structure, but it can be also used independently as a phased array. The array has an oval-shaped rim to maximize the efficiency of the HA, and is composed of 20 horn elements in a hexagonal structure. The element has a horn radiator with a conical helix, which is placed inside the horn and excited by two ports for TX and RX at both ends. Therefore, the antenna can be simultaneously operational in the Ka-band TX and K-band RX frequency bands, using a compact structure providing left-hand circular polarization (LHCP) for TX and right-hand circular polarization (RHCP) for RX. The fabricated array is connected with active channel modules having 20 channels each for TX and RX, and it was experimented on within a beam scanning range of -5° to $+5^{\circ}$ in the azimuth and elevation directions using phase control of the active channel module. The antenna has a minimum gain of 21.7 dBi over the TX band and 19.7 dBi over the RX band over the desired scan region. The maximum pointing error is about 0.32° and the pointing loss is approximately 1.3 dB. In addition to meeting the above RF requirements, the antenna is designed to meet environmental specifications such as wind loads as required for mobile terminals.**

***Index Terms*—Antenna array heed, helix, dual-band, dual polarization.**

I. Introduction

In this paper, a horn array antenna that can be used as a feeder for an HA is introduced [1], [2]. HAs are adopted for the structures of mobile terminals to provide operationality at the Ka-band Tx and K-band RX with dual-circular polarization capability as well as to allow communications with geo-stationary satellites. Reflector antennas of C- and Ku-band satellite communication systems with single dual-mode feeds generally employ horns used in conjunction with pintle hooks, polarizers, and orthomode transducers based on circular or square waveguides. However, such feeds have large transverse dimensions (2 to 3λ), and thus they cannot be used as array elements, as the element spacing should be no greater than 1 to 1.5λ. Most studies on dual-band radiators with circular polarization have been conducted at low frequencies [3], [4], while studies at high frequencies have focused on the realization of high efficiency with limited performance [5]. Therefore, it has been suggested that a dual-band and dual-polarized horn antenna structure having a conical helix as an exiter be used [6]. The antenna's main defect is that it is difficult to fabricate owing to the helix and dielectic cone supporting it. A helix can be made by winding metal wire around the cone.

Manuscript received October 29, 2010; revised June 17, 2011, August 05, 2011; accepted August 16, 2011. Date of publication December 16, 2011; date of current version March 02, 2012. This work was supported by the Basic Science Research Program through the National Research Foundation of Korea(NRF) funded by the Ministry of Education, Science and Technology (2011-0013213).

Y. B. Jung is with Hanbat National University, Daejeon, South Korea (e-mail: ybjung@hanbat.ac.kr).

S. Y. Eom is with Electronics and Telecommunications Research Institute (ETRI), Daejeon, South Korea (e-mail: syeom@etri.re.kr).

Color versions of one or more of the figures in this paper are available online at http://ieeexplore.ieee.org

Digital Object Identifier 10.1109/TAP.2011.2180311

TABLE I
MAIN SPECIFICATIONS OF THE ARRAY

Parameter	TX	RX
Frequency	30.085 – 30.885 GHz	20.355 – 21.155 GHz
Polarization	LHCP	RHCP
Return loss	> 10 dB	> 10 dB
Axial ratio on axis	< 1 dB	< 1 dB
Isolation	> 15 dB (for RX band)	> 10 dB (for TX band)

In this paper, a modified horn antenna with a helix is introduced. This antenna has almost the same structure as the antenna mentioned above, but it has no dielectric cone to support the helix. The helix was substituted with a helical compressive spring made of carbon steel for strengthened elasticity. Thus, the horn antenna is easy to fabricate and its production costs can be considerably reduced.

An array design using the modified horn antenna is described in detail here. The array is composed of 20 elements in the aperture rim with a distorted oval shape to optimize the HA performance in a given size, and the element antennas are rotated by 90° for optimal beam pattern synthesis. The main specifications of the array are summarized in Table I.

II. Design of Horn Antenna With Helix Exciter

A. Design Concept of the Horn Antenna

To develop an array operating in dual bands with dual polarization, the design of the element antenna is essential. To realize an element antenna that meets the array antenna performance requirements listed in Table I in a small-sized structure, a horn antenna with a cone-type helix having two ports at both ends is proposed. The structural design is shown in Fig. 1.

The helix is excited by two semi-rigid coaxial cables placed at the center (port 1) and edge (port 2) of the bottom plate of the horn. The cable at port 1 excites the helix by the transmitter

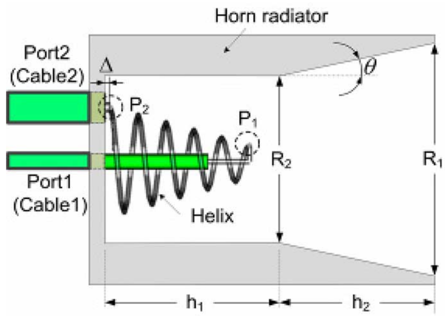

(a)

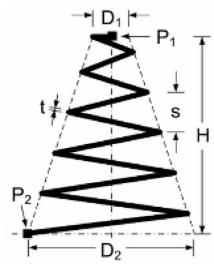

(b)

Fig. 1. Design of a horn antenna with helix exciter: (a) horn antenna structure and (b) geometry of the helix exciter.

signals within a band of 30.085 to 30.885 GHz. The cable is connected to the helix at the top, and it excites the current flowing from the top to the bottom of the helix [6]. This current excites the so-called backward waveguide mode of the first type, T_{-1}, of the circular polarization, which propagates toward the horn direction. Because the current spirals in the right-handed direction from the top to bottom of the helix, the mode has a right-handed rotation. The mode is then reflected at the bottom of the horn in the opposite direction, and the mode reverses to the left-handed rotation, i.e., LHCP.

The other cable at port 2 is intended to receive signals coming to the horn within a band of 20.355 to 21.155 GHz. These signals in the form of a right-handed polarized wave excite the current at the bottom part of the helix, where cable 2 is connected. Consequently, the RX signal excites at the bottom of the helix, P_2, and has RHCP, which is the forward mode of the first type T_1, the so-called axial mode [6].

B. Desigin of Helix Exciter

The main design parameters for the helix exciter are presented in Fig. 1(a). The ends of the helix, P1 and P2, are interconnected with cables 1 and 2, and the design parameters determining the electromagnetic characteristics of the exciter are as follows: D_1 is the top diameter of the helix, D_2 is the bottom diameter of the helix, H is the axial length of the helix, s is the space between the turns, $\mathrm{N} = \mathrm{H}/\mathrm{s}$ is the number of the turns, and t is the diameter of the helix wire.

For a preliminary determination of the helix dimensions, it is necessary to find such parameters as the spacing between the turns, s, the helix top diameter, D_1, and the helix bottom diameter, D_2. These parameters provide the existence of the backward mode of the first type T_{-1} in the Ka-band, and the forward mode of the first type T_1 in the K-band. Therefore, the parameter relation for the T_{-1} and T_1 modes affecting the excitation is used depending on the helix radius R, wavelength λ, and helix pitch angle α. The angle α is related to the helix turn spacing s by

$$\alpha = \frac{180}{\pi} \tan^{-1}\left(\frac{S}{2\pi R}\right) \text{ [degree]}. \quad (1)$$

For excitation of the T_{-1} mode at $\mathrm{f}_{\mathrm{TX}} = 30$ GHz ($\lambda_{\mathrm{TX}} = 1$ cm) for $\alpha = 12^\circ$, we find that $2\pi\mathrm{R}/\lambda_{\mathrm{TX}} \approx 0.75$. Therefore, the top helix diameter is $\mathrm{D}_1 \approx 1.2$ mm and the turn spacing is $\mathrm{s} = 2\pi\mathrm{R} \times \tan 12^\circ = 1.6$ mm. If we now consider a conical helix with constant turn spacing s, then, for effective T_1 mode excitation at the bottom of the helix with a receiver frequency of $\mathrm{f}_{\mathrm{RX}} = 21$ GHz ($\lambda_{\mathrm{RX}} = 1.43$ cm), it is necessary to choose a helix diameter with a condition of $\pi\mathrm{D}/\lambda_{\mathrm{RX}} \approx 1.0$; therefore $\mathrm{D}_2 \approx 4.8$ mm.

In the process of optimizing the exciter characteristics using *CST Microwave Studio®*, the helix and waveguide dimensions above, as well as the number of helix turns N, have been changed to achieve the specified exciter characteristics such as axial-ratio and impedance characteristics.

Generally, the polarization characteristics of helical antennas are improved by increasing the number of turns. Moreover, with a smaller number of turns, the radiator fabrication becomes accordingly simpler. Based on a parameter simulation of the helix, the number of helix turns N should be more than 5 in order to achieve an axial ratio performance lower than 1 dB.

For the axial mode of a helix antenna with uniform spacing between turns, the following empirical expression of terminal impedance may be used

$$Z_{\text{input}} \approx 140 \frac{2\pi R}{\lambda} \; [\Omega]. \quad (2)$$

C. Simulation and Fabrication of Horn Antenna

A performance optimization of the horn antenna with a helix exciter, including the reflection characteristic and antenna gain, was performed using *CST Microwave Studio®* for the 2-port model shown in Fig. 1(b). According to the results of the simulation, the final design parameters of the helix exciter were decided as $\mathrm{D}_1 = 2.0$ mm, $\mathrm{D}_2 = 6.3$ mm, $\mathrm{s} = 1.6$ mm, $\mathrm{H} = 8$ mm, $\mathrm{N} = 5$, and $\mathrm{t} = 0.4$ mm. The horn design was also determined through calculations and a simulation so as to maximize the antenna performance, particularly the isolation between the TX and RX ports. To this end, the following results were obtained: $\mathrm{R}_1 = 14$ mm, $\mathrm{R}_2 = 10$ mm, $\mathrm{h}_1 = 13$ mm, $\mathrm{h}_2 = 10$ mm, and $\theta = 11^\circ$. For matching Port 1, a transformer formed by a piece of cable 1, which is 1.6 mm in length and has no Teflon filling, was used. The matching of Port 2 is achieved using a stub placed near the connection point, P_2, of the helix and cable 2. The best matching of Port 2 was achieved when the distance between the bottom of the horn and the helix equals $\Delta = 0.3$ mm.

The horn antenna was fabricated and tested. The horn is made of aluminum, and the helix was substituted with a helical compressive spring made of carbon steel with strengthened elasticity. To verify the suitability of the helical compressive spring

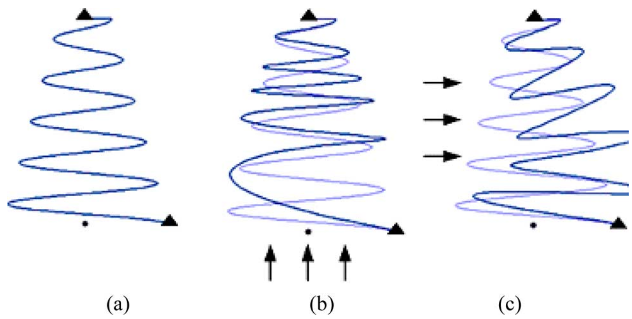

Fig. 2. Loads on conical compressive spring: (a) stable state, (b) vertical load, and (c) horizontal load.

without a dielectic cone, an analysis of a helix mechanical model under static and dynamic loads was performed using the simulation software *NASTRAN*® from MSC, Inc.

A conical spring fixed rigidly at the end points, P_1 and P_2, shown in Fig. 1, has been used as a mechanical model. The spring is assumed to be a metal wire 0.4 mm in diameter with the following characteristics: a mass density of $\rho = 8.94$ g/cm^3, Young's modulus of $\mathrm{E} = 11.5\ 10^4$ MPa, shear modulus of $\mathrm{G} = 4.24\ 10^4$ MPa, and ultimate fluidity stress limit of $\sigma =$ 300 MPa. The calculations have been performed under external static loads caused by 10 g acceleration, as well as external dynamic loads under general vibration and impact characteristics.

Fig. 2 shows the mechanical simulation results. Under a static load of 10 g, the deformations of the helix are smaller than 0.01 mm, and the mechanical stress does not exceed 2 MPa. Such deformations have little effect on the main electrical performances of the exciter in general situations, and the helix cannot be destroyed by external effects or stresses that can arise in moving vehicles. Therefore, by the adoption of a helical compressive spring, the horn antenna is very easy to fabricate, and the production costs can be considerably reduced.

The measured results of the horn antenna are shown in Fig. 3. From the results, it can be seen that the horn antenna has gains of 11.2 and 8.6 dBi in the TX and RX, respectively. The antenna has a minimum return loss of 15.2 dB for TX and 13.4 dB for RX, and the minimum isolation performance is 22.8 dB and 26.2 dB for TX and RX, respectively. The axial ratio in the broadside direction is less than 1 dB in both the TX and RX bands. It can be observed that the radiation pattern is displaced by 10° in the TX due to multimode generation in the horn. The TX and RX phased ceneters are located 10.5 cm and 9.8 cm behind the horn aperture, respectively. As explained above, the element antenna with conical helix has a complicated operation mechanism for dual-band and dual polarization characteristic. Furthermore, the antenna fabrication error and assembly condition can adversely affect the antenna performance, especially return loss and port isolation.

III. Feed Horn Array Design

A. Array Structure Analysis

To enhance the antenna performances, particularly the antenna gain, the easiest method is to increase the reflector size.

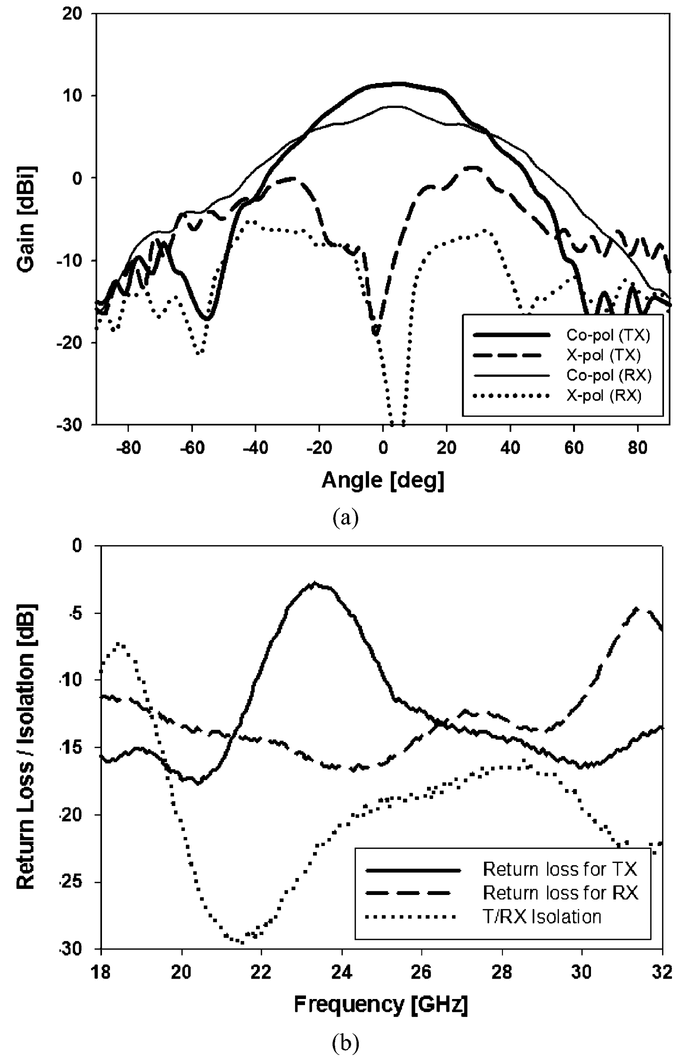

Fig. 3. Measured results of element antenna: (a) elevation radiation pattern and (b) return loss and isolaton.

For this purpose, we can use an elliptical reflector aperture in the HA design. This solution is very attractive because the performance can be enhanced without any changes of the maximum dimensions of the HA.

In this case, one difficulty concerning the elliptical reflector aperture is the need for a special array aperture with a distorted oval shape to obtain an acceptable field distribution on the main reflector. If we choose an array with a general aperture shape (rectangular or circular), the overall performance of the HA may be degraded. Performance degradation can arise from spillover of radiated power from the array to the reflector. In addition, poor aperture efficiency can occur when the radiated power from the array is smaller than the aperture size of the reflector.

In order to design the array, the total number of array elements should first be selected. In this design, the maximum number of antenna elements in the array was 20, as determined in the structural design step of the HA. In the next step, we analyzed two possible versions of the array lattice. In the first version, the array consists of a hexagonal lattice of conical horns, while in the second the array is a triangular lattice of square horns. We conducted simulations for both versions. Taking into account

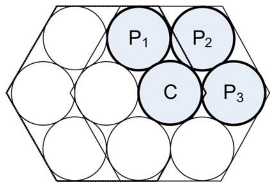

Fig. 4. 10-radiator hexagonal model of array.

the features of the array construction, we assumed that the size of the horn aperture is 14 mm, and that the diameter of each horn input is 10 mm, in accordance with the simulation and modeling results of the helical exciter. The most suitable element spacing is 15 mm, which can be considered to be 0.76 λ_0 and 0.54 λ_0 for the TX and RX bands at the center frequency of the operation band in the hexagonal structure. Based on the simulation, it was demonstrated that the gain of the square horn model is greater than that of the conical horn by 0.2 and 0.5 dB in the TX and RX bands, respectively. However, the gain difference of the elements has a weak influence of about 0.2 dB on the gain characteristic of the HA, and the fabrication of the array based on the square horns is very complicated. The general mechanical processing for a square horn, particularly at right angles, cannot provide the required precision for mm-waves, which can be a major factor leading to high production costs. Thus, the conical horn was chosen as the element for the array with a hexagonal lattice.

B. Compensation of Radiation Pattern

Fig. 4 shows a 10-radiator hexagonal model that consists of two hexagonal models. This model is used for a more detailed simulation analysis of the radiation characteristics of the conical horn elements embedded in the hexagonal structure which are formed by placing elements in the equilateral triangular grid with same spacing. The array spacing was determined to get optimum performance, especially array gain and radiation pattern. In simulating the array, the amplitude and phase characteristics of the central and periphery elements of a 10-radiator hexagonal model are estimated. In Fig. 4, the sample array elements are denoted as C, P_1, P_2, and P_3. The element C is the typical center positioned array element and P_1, P_2, and P_3 are the sample elements positioned at the edge of the array structure. Other elements of the fragment have similar characteristics due to the geometrical symetry.

The simulated radiation patterns of the elements are presented in Fig. 5. From the results, it can be confirmed that all of the elements have similar characteristics. However, we can ascertain that the radiation patterns for the TX in the azimuth are deflected from the zero direction by -5°. In the conical horn structure, two orthogonal modes are created by the exciter at the horn input in the RX. However, hybrid modes similar to the TE_{11} and TE_{21} modes of an unloaded circular waveguide are excited in the TX, and the radiation patterns are tilted from 0° by these modes.

In this array design,

To compensate the deflection of the radiation pattern in the array, it is expedient to turn the exciters at the element inputs, within a limit of 0° to 270°, with angle steps of 90°. On the other hand, it is desirable to provide a mirror phase distribution in the sub-arrays of the adjacent tracking channels. A variant of the exciter arrangement is shown in Fig. 6(a). The initial phase distribution in the array caused by the helical exciter can be compensated by means of the phase shifters in the active channels through calibration of the antenna.

C. Tracking Beam Synthesis

The proposed array has a satellite tracking capability, allowing it to be loaded into mobile satellite terminals. The primary role of the tracking function is to provide a stable communication service using permanent beam pointing toward the target satellite under vehicle movement. Various studies on the tracking function have been reported in the literature, including manual/programmed beam steering, mono-pulse tracking, sequential amplitude sensing by conical scan and step tracking, and electronic beam squinting [7]. The latter three techniques can be classified as auto-tracking, the representative approach for closed-loop tracking systems. Once the satellite acquisitions have been established, the tracking process is continually accomplished by the tracking algorithm. All auto-tracking schemes rely on the reception of a continuous pilot signal transmitted by the satellite. The received satellite signal is then used to derive the pointing error information.

The array uses a sequential amplitude sensing method for satellite tracking. The tracking beam is made by the RX beam pattern at the K-band. For tracking beam formation, we divided the array into five groups, as shown in Fig. 6(a). Each group is composed of four element antennas; their electrical center points are slightly different because the rim (e.g., shape) of the array is asymmetrical in the Y-axis. Within the groups, Group 2 is not used to form the tracking beam for gain symmetry.

Fig. 6(b) shows the tracking beam location. The HA continuously creates four spot beams for tracking, accomplished by means of five phase-shifters connected to each array group.

IV. Fabrication and Performance Test

The fabricated array prototype is shown in Fig. 7. The array consists of a matrix of 20 conical radiators realized as holes in a metallic plate, while helix exciters are fabricated with the bottom side of the horns. In the assembly, 20 exciters are individually inserted into the horn structure with 20 conical radiators, and these exciters can be tightly assembled using a few screws.

The fabricated array was measured using a far field measurement system from *Orbit/FR, Inc.*, in an anechoic chamber. To confirm the capability to control the antenna beams, 20 active channels were connected next to the array. The active channels were composed of several components, such as amplifiers, variable attenuators, and phase shifters. By using the active channels, the main roles of the array, such as control of the radiated power and antenna beam pointing, including the selection of TX and RX, can be realized.

The measured radiation patterns of the array are depicted in Fig. 8. The figure shows the radiation pattern of the main beam at a pointing $\text{angle} = 0^\circ$, with the tracking beams tilted by $\pm 5^\circ$ in

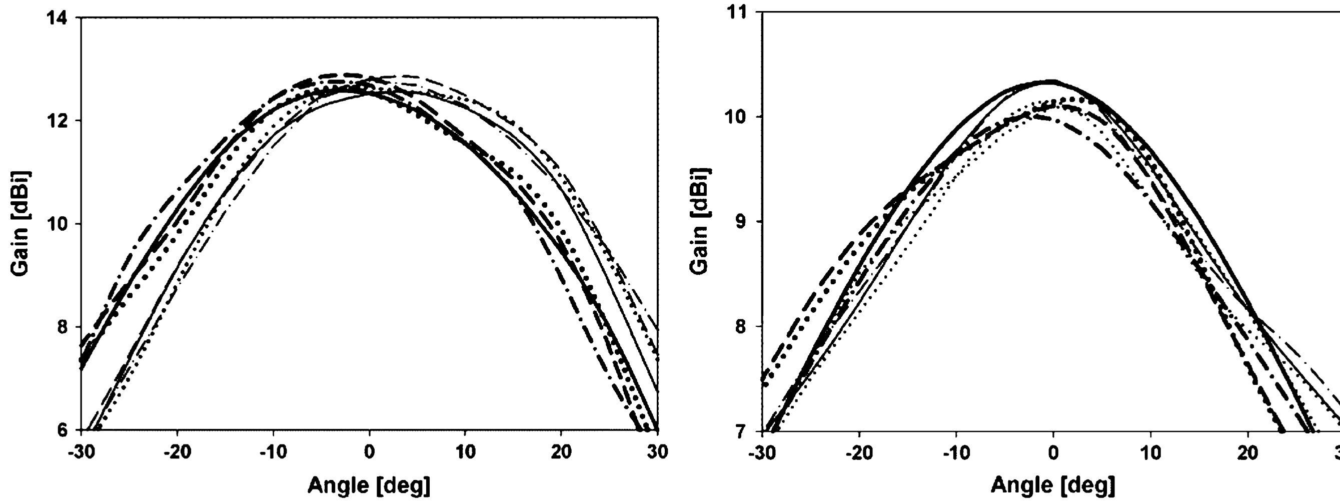

(a) (b)

Fig. 5. Simulated radiation pattern analysis of the elements in hexagonal model: (a) TX-band (b) RX-band (—— Azimuth for ‘1’, - - - - Azimuth for ‘A’, ... Azimuth for ‘E’, -·-·-· Azimuth for ‘C’, ▬ Elevation for ‘1’, ▬ ▬ Elevation for ‘A’, ... Elevation for ‘E’, ▬·· Elevation for ‘C’).

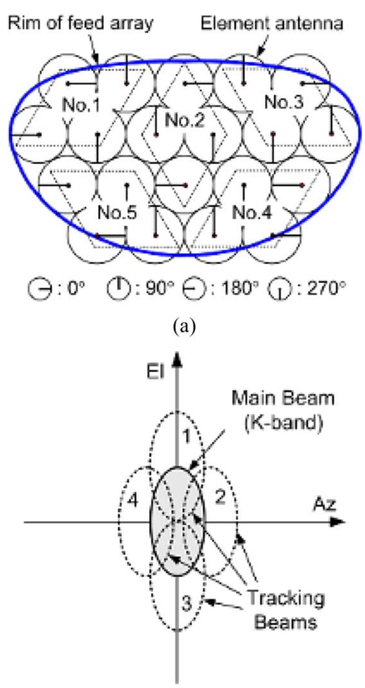

(b)

Fig. 6. Arrangement of the array and tracking beam control method: (a) initial phase and group assignment of array for tracking beam control, and (b) tracking beam location.

the azimuth and elevation directions. At a beam scanning angle of 0°, the array has minimum gains of 22.7 and 20.6 dBi for TX and RX, respectively. The side-lobe level characteristic in the azimuth direction is better than that in the elevation direction, because more element antennas are placed in azimuth. The side-lobe levels are 13.5 and 19.4 dB for the TX and RX, respectively. Moreover, the minimum gains of the array at a beam scanning angle of $\pm 5^\circ$ are 10.5 and 11.8 dBi for the TX and RX, respectively. The side-lobe levels are also about 10.5 and 11.8 dB for TX and RX. The array has a pointing error of 0.32° and

Fig. 7. Fabricated array prototype.

a maximum pointing loss of 1.3 dB. With the structural shape of the array, the characteristic difference among the active channels is the main reason for performance deterioration, resulting in pointing loss and pointing error.

V. Conclusion

This paper introduces a horn array that can be loaded into mobile satellite terminals with an HA structure. The array is composed of 20 elements in the aperture rim in a distorted oval shape to optimize the HA performance in a given size. For bilateral satellite communications, the array can be operated in the Ka-band (30.085 to 30.885 GHz) for TX and in the K-band (20.355 to 21.155 GHz) for RX, and provides left-hand circular polarization (LHCP) in TX and right-hand circular polarization (RHCP) in RX.

To realize an array that meets the performance results noted above, a horn antenna including a conical helix is introduced. The helix can be excited using two ports for TX and RX at both ends, and it was fabricated with a helical compressive spring having good elasticity. Owing to its structural characteristics, the horn antenna can be easily fabricated at low production costs. Simulations and measurements reveal that the horn element performs well and meets the required specifications. However, its radiation pattern is tilted by about 5° in TX by the

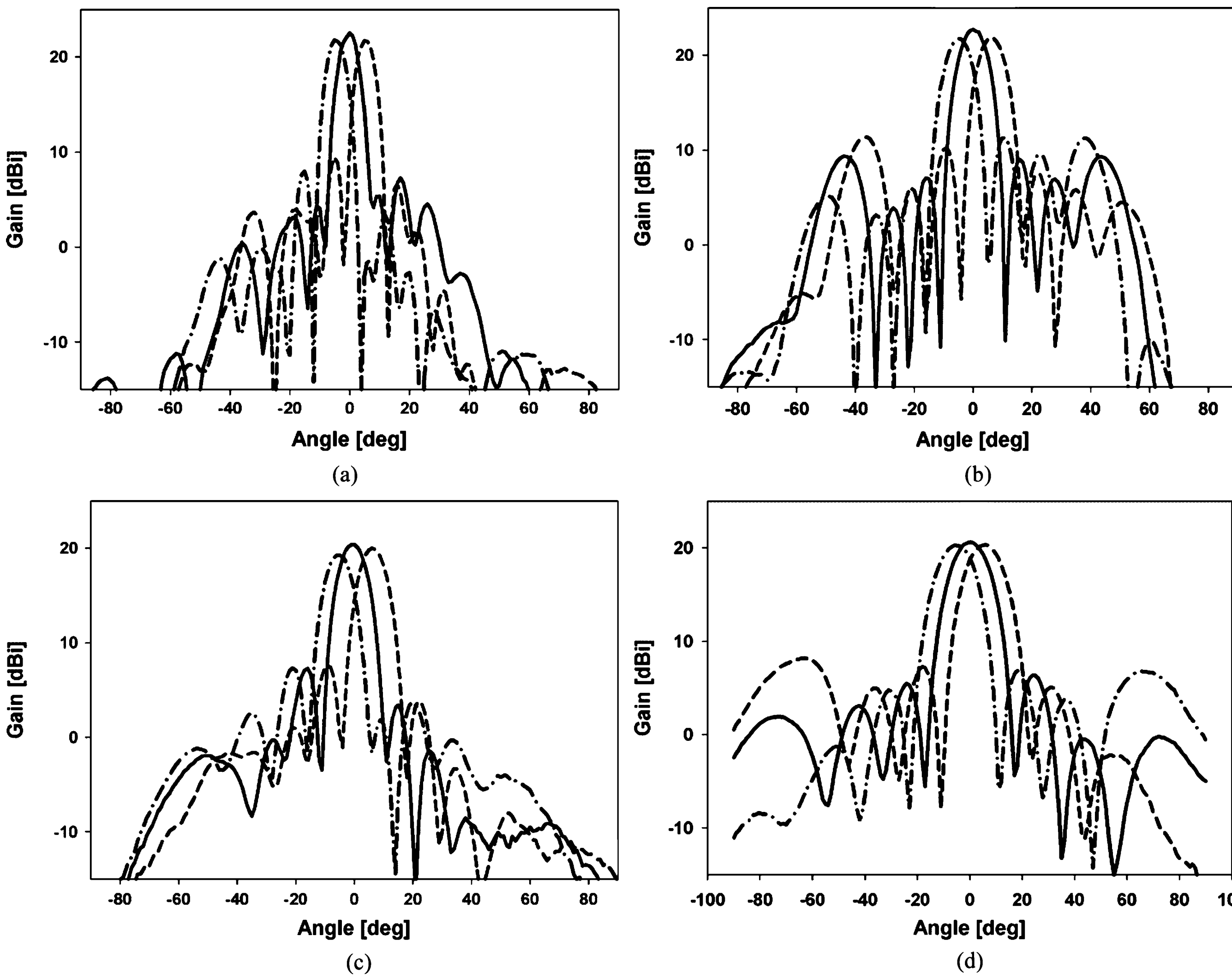

Fig. 8. Measured radiation patterns of the array: (a) azimuth direction in TX, (b) elevations direction in TX, (c) azimuth direction in RX, and (d) elevation direction in RX (—— 0°, - - - - $+5°$, -.-.-. $-5°$).

higher-order modes. To compensate for the deflection of the radiation pattern in the array, the helix exciters are adjusted to obtain a phase of 0° to 270° with angle steps of 90°. Using the active channels for satellite tracking, the array has capacity for beam pointing control in a range of $+5°$ to -5.

Based on the performance tests, we have confirmed that the fabricated array shows optimal performance in an HA structure having a special shape for the reflector. With the use of circular polarization, the proposed structure of the horn element is expected to find extensive use in satellite communications.

Acknowledgment

The authors would like to thank S. I. Jeon, A. V. Shishlov, S. Ganin, and other members of ETRI and JSC APEX for their valuable advice and contributions to the array design.

References

[1] Y. B. Jung, A. V. Shishlov, and S. O. Park, "Cassegrain antenna with hybrid beam steering scheme for mobile satellite communications," *IEEE Trans. Antenna Propagat.*, vol. 57, no. 5, pp. 1367–1372, May 2009.

[2] Y. B. Jung and S. O. ParkS, "Ka-band shaped reflector hybrid antenna illuminated by microstrip-fed horn array," *IEEE Trans. Antenna Propagat.*, vol. 56, no. 12, pp. 3863–3867, Dec. 2008.

[3] K. P. Yang and K. L. Wong, "Dual-band circularly-polarized square microstrip antenna," *IEEE Trans. Antenna Propagat.*, vol. 49, no. 3, pp. 377–382, Mar. 2001.

[4] Y. J. Sung and Y. S. Kim, "Circular polarised microstrip patch antennas for broadband and dual-band operation," *Electron. Lett.*, vol. 40, no. 9, pp. 520–522, Apr. 2004.

[5] Y. B. Jung, S. Y. Eom, S. I. Jeon, and C. J. Kim, "Novel Ka-band microstrip antenna fed circular polarized horn array antenna," in *IEEE Int. Symp. Antenna and Propagation*, Pasadena, CA, Jun. 2004.

[6] Y. B. Jung, S. Y. Eom, S. I. Jeon, and S. O. Park, "Dual-band and dual-polarized horn antenna including conical helix," *Electron. Lett.*, vol. 43, no. 8, pp. 432–434, Apr. 2007.

[7] J. L. Volakis, R. C. Johnson, and H. Jasik, *Antenna Engineering Handbook*, 4th ed. New York: McGraw-Hill, 2007, ch. 42.

[8] K. R. Carver, "The helicone—A circularly polarized antenna with low sidelobe level," *Proc. IEEE*, vol. 55, no. 4, p. 559, Apr. 1967.

[9] M.-S. Lee, "Wideband capon beamforming for a planar phased radar array with antenna switching," *ETRI J.*, vol. 31, no. 3, pp. 321–323, June 2009.

Young-Bae Jung (M'09) was born in Seoul, Korea. He received the B.S. in radio science and engineering from KwangWoon University, Seoul, Korea, in 1999, the M.S. and the Ph.D. degrees in information and communications engineering from Korea Advanced Institute of Science and Technology (KAIST), Daejeon, Korea, in 2001 and 2009, respectively.

From 2001 to 2011, he was with Electronics and Telecommunications Research Institute (ETRI), Daejeon, Korea, as a Senior Researcher. From March 2011, he is a Professor in the division of electric, electronic and control engineering, Hanbat National University, Daejeon, Korea. His research interests include active phased array antenna systems, radars and active/passive components in the field of RF and Microwave.

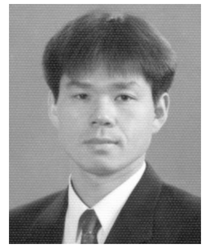

Soon-Young Eom (M'01) was born in Gangwon-do, Korea, on May 2, 1964. He received the B.S. and M.S. degrees in electronic engineering from Yonsei University, Seoul, Korea, in 1988 and 1990 respectively. With the study on flat-topped radiation pattern using a multi-layered disk array structure, he received the Ph.D. degree in electronic engineering from Yonsei University, Seoul, Korea, in 2003.

Since 1990, he has worked at Electronics and Telecommunications Research Institute (ETRI), Daejeon, Korea, as a Principal Member of the research staff. From 1991 to 1993, he participated in the joint project with Alenia Spazio S.P.A in Italy, for developing the very small aperture terminal (VSAT) system. From 1996 to 2006, he took part in developing many mobile active phased array antenna systems for direct broadcasting satellite (DBS) reception and satellite communications. Also, he developed the multi-mode(frequency) reconfigurable array antenna system and polarization reconfigurable array antenna system for future mobile communications from 2007 to 2010. From September 2009, he has served as an Adjunct Professor in the Department of Mobile Communication and Digital Broadcasting Engineering at the University of Science & Technology (UST), Daejeon, Korea. His research interests include active phased array antenna systems, microwave circuits and systems, and advanced mobile base station antenna systems.